PHYSICAL REVIEW B VOLUME 24, NUMBER 2 15 JULY 1981

Full-potential self-consistent linearized-augmented-plane-wave method for calculating the electronic structure of molecules and surfaces: O_2 molecule

E. Wimmer*
Department of Physics and Astronomy, Northwestern University, Evanston, Illinois 60201

H. Krakauer
Department of Physics, College of William and Mary, Williamsburg, Virginia 23185

M. Weinert
Department of Physics and Astronomy and Materials Research Center, Northwestern University, Evanston, Illinois 60201

A. J. Freeman
Department of Physics and Astronomy and Materials Research Center, Northwestern University, Evanston, Illinois 60201 and Argonne National Laboratory, Argonne, Illinois 60439
(Received 19 February 1981)

The linearized-augmented-plane-wave (LAPW) method for thin films is generalized by removing the remaining shape approximation to the potential inside the atomic spheres. A new technique for solving Poisson's equation for a general charge density and potential is described and implemented in the film LAPW method. In the resulting full-potential LAPW method (FLAPW), all contributions to the potential are completely taken into account in the Hamiltonian matrix elements. The accuracy of the method—already well known for clean metal surfaces—is demonstrated for the case of a nearly free (noninteracting) O_2 molecule which is a severe test case of the method because of its large anisotropic charge distribution. Detailed comparisons show that the accuracy of the FLAPW results for O_2 exceeds that of existing state-of-the-art local-density linear-combination-of-atomic-orbitals (LCAO)-type calculations, and that taking the full potential LAPW results as a reference, the LCAO basis can be improved by adding off-site functions. Thus the full-potential LAPW is a unified method which is ideally suited to test not only molecular adsorption on surfaces, but also the components of the same system separately, i.e., the extreme limits of the molecule and the clean surface.

I. INTRODUCTION

It is now generally accepted that in-depth knowledge of the electronic structure and properties of adsorbates (atoms and molecules) on transition-metal surfaces is of great scientific and technological importance. In the last decade, intense experimental efforts using advanced techniques for sample preparation and characterization have provided a vast quantity of data. These developments have challenged present theoretical understanding and have encouraged the development of theoretical methods of interpreting the phenomena observed. Thus, in recent years, first-principles energy-band studies of thin films have demonstrated a fair degree of sophistication in tackling a number of complex problems involving the electronic structure of free surfaces (including surface reconstruction and relaxation), chemisorption bonding of atomic adsorbates, and interface phenomena. A principal aim has been to achieve "self-consistency," whose effect on the results is known to be very important for systems which demonstrate a fair degree of charge transfer between atom species. Still, this is but only one part of the challenge, since the two most important characteristics of a first-principles band calculation are the *degree* of self-consistency and the approximations to the potential.

The effect of approximations to the potential, however, depend far more on the systems considered. There are two main approximations made: (1) the (local-density) exchange-correlation approxi-

mation[1] and (2) the shape approximations to the potential. The local-density approximation is the best available today and appears to give fairly good results. On the other hand, the validity of different shape approximations depends strongly on the systems considered. The muffin-tin (MT) and the overlapping spherical atomic charge densities approximations are quite good for close-packed metals, but are suspect for open structures such as semiconductors and reduced symmetry solids, e.g., films and interfaces, and the localization inherent in molecules on solid surfaces.

One of the most successful bulk-slab methods, the self-consistent linearized-augmented-plane-wave (LAPW) method,[2] has been used to treat nearly free-electron and transition-metal surfaces[3–6] and also atomic chemisorption.[7,8] In these LAPW calculations, the full potential and charge density were treated everywhere in space except inside the muffin-tin spheres, where a spherical-shape approximation was used. While these calculations yield accurate results for close-packed metal systems and saturated atomic chemisorption [e.g., $p(1\times1)$ overlayers], a spherical-shape approximation cannot be justified for open semiconductor surfaces or molecular chemisorption when highly accurate solutions to the local- (spin-) density—functional equations are required.

In this paper the remaining MT shape approximation is removed using a new method we have developed for obtaining the Coulomb potential for a general periodic charge distribution without shape approximation. The method is based on the concept of multipole potentials and the Dirichlet problem for a sphere. This is not an Ewald-type method, but rather a new alternative. The basic idea is that the potential outside a localized charge distribution depends on the charge only through the multipole moments.[9,10] In order to obtain the potential in the interstitial region of a crystal, we need to know only the (rapidly convergent) Fourier representation of the smooth interstitial charge density and the multipole moments of the charge in the different spheres. Since multipole moments do not define a unique charge density, we replace the true charge inside the spheres with a pseudo-charge-density of the same multipole moments, but which has a rapidly convergent Fourier representation. This pseudocharge is used to obtain the correct Coulomb potential everywhere in the interstitial and on the spheres. We then obtain the potential inside the spheres by solving the boundary-value problem using the true charge density in this region.

The resulting full-potential LAPW method (FLAPW) may be used, in principle, to treat all surfaces and chemisorption system, limited only by available computer resources. Therefore, the FLAPW method is a unified method capable of treating not only molecular absorption on surfaces, but also the extreme limits of the isolated molecule and the clean surface.

II. METHOD OF CALCULATION

The present method is a generalization of the previously described film LAPW method.[3] The generalization is achieved by relaxing the remaining muffin-tin approximation in the potential, i.e., by solving Poisson's equation for the general potential and by including the Hamiltonian matrix elements due to nonspherical terms of the potential inside the muffin-tin spheres. This section describes the implementation of the newly developed method[9,10] of solving Poisson's equation for periodic structures for the case of the film LAPW method, and the inclusion of the matrix elements due to the nonspherical terms in the potential operator. Although there are no special symmetry requirements, the formulation here is given for a film with inversion and z reflection, as in Ref. 3.

A. Solution of Poisson's equation

The charge density is given by

$$\rho(\vec{r})=\begin{cases}\sum\rho_\nu(r_\alpha)K_\nu(\hat{r}_\alpha)-2Z_\alpha\delta(\vec{r}_\alpha) & \text{inside sphere } \alpha \quad (1a)\\ \sum\limits_{n,s}\rho^{\mathrm{PW}}_{n,s}\cos(k_nz)\Phi_s(\vec{r}) & \text{in the interstitial} \quad (1b)\\ \sum\limits_{s}\rho_s(z)\Phi_s(\vec{r}) & \text{in the vacuum} \quad , \quad (1c)\end{cases}$$

where

$$K_\nu(\hat{r})=\sum_m c_m(\nu)Y_{l_\nu m}(\hat{r}) \quad (2)$$

is a lattice harmonic, $\vec{r}_\alpha=\vec{r}-\vec{\tau}_\alpha$, $\vec{\tau}_\alpha$ is the position of the atomic sphere α, and $\Phi_s(\vec{r})$ is a two-dimensional (2D) plane-wave star function

$$\Phi_s(\vec{r})=\frac{1}{n_0}\sum_R\exp[i\hat{R}\vec{G}_s\cdot(\vec{r}-\vec{t}_R)] \quad , \quad (3)$$

where $\vec{G}_s$ is a 2D star representative reciprocal-

lattice vector, $\hat{R}$ is the point-group part of the 2D space group operation R, $\vec{t}_R$ is a nonprimitive 2D translation vector, and n_0 is the number of 2D space-group operations, e.g., 12 for the hexagonal lattice.

Poisson's equation can be solved in a straightforward manner[11,4] once the charge density is expressed as

$$\rho(\vec{r}) = \sum_s \rho_s(z)\Phi_s(\vec{r}) \quad . \tag{4}$$

However, because of the rapid variation of the charge density near the nuclei, a Fourier expansion of the form (4) for the charge density in the MT sphere would be extremely slowly convergent. The representation of the charge density in the interstitial and vacuum region [see Eq. (1)] already has the desired form given by Eq. (4).

In order to treat the region inside the muffin-tin spheres correctly, we follow a variant of the scheme used by Hamann[9] as discussed by Weinert.[10] This scheme is based on the fact that the potential outside the muffin-tin spheres does not depend on the actual shape of the charge density inside the spheres but only on the multipole moments of this charge. Hence, we can replace the true rapidly varying charge inside the MT spheres by another, smoother charge (referred to as the full pseudo-charge-density) without changing the potential outside the spheres if the full pseudo-charge-density is required to have the correct multipole moments. A rapidly convergent Fourier expansion of this smooth pseudocharge can be obtained and the charge density can therefore be expressed in the desired form [Eq. (4)]. Now Poisson's equation can be solved giving the correct value of the potential everywhere outside the spheres, and in particular on the sphere boundaries. We then find the expansion in lattice harmonics of this potential on the sphere boundaries. In a final step the lattice harmonics expansion of the potential inside the spheres is found by a Green's-function method from the original charge density using the now known potential on the sphere as a boundary condition.

Actually, the replacement of the original charge density by a smooth pseudocharge inside the spheres is done in two steps: (1) The expansion (1b) of the charge density in the interstitial region, $\rho^{\mathrm{PW}}(\vec{r})$, is extended into the muffin-tin spheres. This charge density already has, of course, the desired Fourier representation. (2) The difference charge density

$$\Delta\rho(\vec{r}) = \rho(\vec{r}) - \rho^{\mathrm{PW}}(\vec{r}) \tag{5}$$

for $\vec{r}$ inside sphere α is replaced by a smooth charge density $\Delta\tilde{\rho}(\vec{r})$ (the difference pseudo-charge-density), which has the same multipole moments as $\Delta\rho(\vec{r})$.

The form of the 2D star-function expansion coefficients of the difference pseudo-charge-density $\Delta\tilde{\rho}(\vec{r})$ is found by using Eq. (28) of Ref. 10 for the 2D star representation of a plane-wave charge density (1b) as used in the present calculation. We then have the desired form of the charge density [Eq. (4)],

$$\tilde{\rho}(\vec{r}) = \sum_s \tilde{\rho}_s(z)\Phi_s(\vec{r}) \tag{6}$$

with

$$\tilde{\rho}_s(z) = \sum_n \tilde{\rho}_{n,s}\cos(k_n z) \quad , \tag{7}$$

$$\tilde{\rho}_{n,s} = \rho_{n,s}^{\mathrm{PW}} + \Delta\tilde{\rho}_{n,s} \quad , \tag{8}$$

where the coefficients $\Delta\tilde{\rho}_{n,s}$ depend on the multipole moments of the original charge q_{lm}^{α}, and the multipole moments of the plane-wave charge inside the spheres, $q_{lm}^{\mathrm{PW}\alpha}$:

$$\Delta\tilde{\rho}_{n,s} = f(q_{lm}^{\alpha} - q_{lm}^{\mathrm{PW}\alpha}) \quad . \tag{9}$$

The explicit form of $\Delta\tilde{\rho}_{n,s}$ is given in the Appendix.

Following Posternak *et al.*,[4] we finally obtain for the Coulomb potential in the interstitial the expression

$$V_C(\vec{r}) = \sum_{n,s} \tilde{V}_{n,s}\cos(k_n z)\Phi_s(\vec{r}) + \sum_{s\neq 0} d_s \cosh(G_s z)\Phi_s(\vec{r}) \quad . \tag{10}$$

Using the expansion of a plane wave with complex $\vec{k}$ in spherical harmonics,[10] we can find the analytic form of the lattice harmonics expansion of the Coulomb potential on a sphere boundary. The Coulomb potential inside the spheres is found from the Coulomb potential on the sphere boundary and the original charge density by using a standard Green's-function method.[12]

B. The total potential

In the interstitial region, a 3D star-function expansion of the exchange-correlation potential is found by a least-squares fit of this potential together with the cosh terms in the Coulomb potential [Eq. (10)]. In the vacuum region and in the region inside the MT spheres, a least-squares fit of the exchange-correlation potential is performed to obtain a 2D star-function expansion and a lattice harmonics expansion, respectively.

Finally, we have a representation of the total potential analogous to the total charge density as follows:

$$V(\vec{r}) = \begin{cases} \sum_{\nu} V_{\nu}(r_\alpha) K_{\nu}(\hat{r}_\alpha) & \text{inside sphere } \alpha \quad (11a) \\ \sum_{n,s} V_{n,s}^{\mathrm{PW}} \cos(k_n z) \Phi_s(\vec{r}) & \text{in the interstitial} \quad (11b) \\ \sum_{s} V_s(z) \Phi_s(\vec{r}) & \text{in the vacuum.} \quad (11c) \end{cases}$$

C. The matrix element ΔH_{NS}

Using the wave function inside a sphere as given by Krakauer *et al.*[3] and taking the nonspherical ($l \neq 0$) terms of the expansion of the total potential [Eq. (11a)], the matrix element ΔH_{NS} is given by

$$\Delta H_{\mathrm{NS}} = \sum_{\alpha} \left\langle \phi_{p'n'}(\vec{k},\vec{r}) \left| \sum_{\nu \neq 0} V_{\nu}(r_\alpha) K_{\nu}(\hat{r}_\alpha) \right| \phi_{pn}(\vec{k},\vec{r}) \right\rangle . \quad (12)$$

This matrix element involves one-dimensional numerical radial integrals of the form

$$\int_0^{R_\alpha} u_{l'}(r,E_l) V_{\nu}(r) u_l(r,E_l) r^2 dr \quad (13)$$

and angle-dependent integrals of the form

$$\int Y_{l'm'}^* Y_{l_\nu m_s} Y_{lm} d\Omega , \quad (14)$$

i.e., Gaunt coefficients. In the present calculation we have used $l',l \leq 4$ and $l_\nu \leq 8$ in evaluating [Eq. (12)]. Although the calculation of the matrix elements [Eq. (12)] is straightforward, particular attention has to be paid to efficient programming because of the many summations involved—$\sum(\alpha,l',m',l_\nu,m_s,l,m)$ for each matrix element. Actually, the time for calculating the matrix elements [Eq. (12)] was less than 25% of the total time for setting up the Hamiltonian matrix.

III. APPLICATION TO THE O_2 MOLECULE

The effect of the nonspherical contributions to the potential obviously plays an important role in the electronic structure of diatomic molecules. Therefore the application of the FLAPW method to such a molecule provides a severe test case. In order to assess the accuracy of the results obtained we will compare it with sophisticated linear-combination-of-atomic-orbitals (LCAO)-type calculations[13,14] using the discrete variational method for free molecules.

A. Computation details

The O_2 molecules are placed in an infinite 2D hexagonal lattice. A spacing of three bondlengths (6.846 a.u.) between molecules was found to be a sufficiently large separation for the limit of noninteracting molecules. The direction of the bonding is normal to the film.

The 1*s* core electrons are treated in the nonrelativistic limit in order to compare with the LCAO-DVM (discrete variational method) results. For the same reason the exchange-correlation potential is approximated by the simple form of the $X\alpha$ potential using $\alpha = 0.7$, a standard value in many DVM calculations.[14] The expansion of the wave functions includes terms with $|\vec{k}| \leq 5.3$ (a.u.$^{-1}$) giving 329 and 275 basis functions for the symmetric and antisymmetric wave functions, respectively. 507 3D stars are used for the expansion of the interstitial charge, the pseudocharge, and the potential in the interstitial. A convergence factor (cf. the Appendix) of $n = 9 - l$ is employed for the 3D star expansion of the difference pseudo-charge-density.[10] The self-consistency cycle was ended when the "distance" between the input and output potentials was less than 2 mRy. By distance we mean the root-mean-square difference

$$d = \left[\frac{1}{\Omega} \int_{\text{unit cell}} [V_{\text{input}}(\vec{r}) - V_{\text{output}}(\vec{r})]^2 d^3r \right]^{1/2} , \quad (15)$$

where Ω is the volume of the unit cell between the vacuum boundaries at $\pm D/2$. A potential mixing scheme suggested by Hamann[9] is employed where the input and output potentials of two previous iterations are used to construct the potential for the next iteration.

B. Total densities and the full potential

The total density, which is of fundamental importance in local- (spin-) density theory, is shown in Fig. 1 as obtained by the FLAPW method for the O_2 molecule. This figure also shows the total valence density and a "plane-wave" density which is obtained when the expansion [Eq. (1b)] is used not only in the interstitial region but also inside the spheres and in the vacuum region. It is interesting

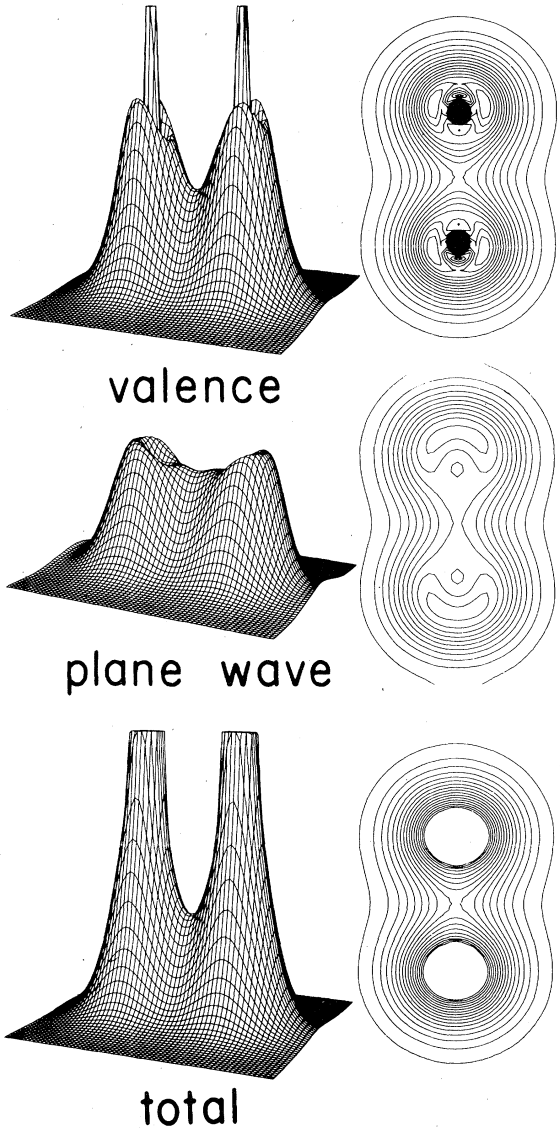

FIG. 1. Valence charge density, extension of the plane-wave charge density into the muffin-tin spheres and into the vacuum, and total FLAPW charge density for the O_2 molecule. All densities are plotted to the same scale. The lowest contour value and the contour spacings are 0.06 electrons/(a.u.)^3.

to note that the continuation of the plane-wave charge into the muffin-tin spheres gives a charge density which is qualitatively similar to the original valence charge density. A quantitative comparison of the difference between the original charge density and the plane-wave continuation is provided by comparing the multipole moments of each density. These moments are tabulated in Table I. (The monopole terms are of opposite sign because the nuclear charge is included in only the original density.) The multipole moments for both densities have the same general trend, but there are substantial differences even for the important small l moments, e.g., the quadropole moments differ by 40%. The effect of these differences when iterating to self-consistency using the plane-wave extension only is not clear and may strongly depend on the system considered.

In this context it should be restated that in the solution of Poisson's equation employed in the FLAPW method, the differences between the multipole moments of the original charge density and those of the plane-wave continuation determine the Fourier coefficients of the difference-pseudo-charge. Then the Fourier representation of the charge density and the boundary-value problem finally lead to the total potential which has no shape approximation. This total potential consisting of the Coulomb potential and the exchange-correlation potential is presented in Fig. 2. From this figure it can be seen that the different representations of this potential as given by Eqs. (11a)–(11c) are converged, since there are no discontinuities across the boundaries in real space between the spheres, the interstitial, and the vacuum regions.

C. One-electron charge densities

Figure 3 presents the single-state densities $P_i(\vec{r}) = \psi_i^*(\vec{r})\psi_i(\vec{r})$. The real-space functions $P_i(\vec{r})$ have the rotational symmetry of the molecule and therefore a cut in a plane containing the two nuclei gives a complete picture of the functions. The densities $P_i(\vec{r})$ are normalized to unity within the two-dimensional unit cell containing just one molecule. For the contour plots (given to the right of each picture) we have chosen an equidistant spacing of the contour lines. Comparison with the Hartree-Fock results of Wahl[15] is difficult to make because he used a quasilogarithmic scale which overemphasizes the low-density regions and suppresses the important structures in the bond region.

As can be seen from Fig. 3, the continuity across the boundaries of the different regions in real space is excellent even for the charge densities of the individual states. Inside the spheres we used lattice harmonics up to $l = 8$ constructed from wave functions of up to $l = 6$, since the contributions from the additional functions with $l = 7$ and $l = 8$ are small for the nonspherical parts of the charge density.

The contour plots given by Kerker *et al.*,[16] as obtained from their self-consistent 3D-supercell

TABLE I. Multipole moments originating from the original charge density ρ and the extended plane-wave charge density ρ^{PW} inside the muffin-tin sphere with radius $R = 1.141$ a.u.

Multipole moment	ρ	ρ^{PW}	Δ (%)
q_{00}	−0.7326	−0.8068	
q_{10}	−0.0128	−0.0110	14
q_{20}	0.0100	0.0140	40
q_{30}	−0.0285	−0.0269	6
q_{40}	0.0123	0.0120	−3

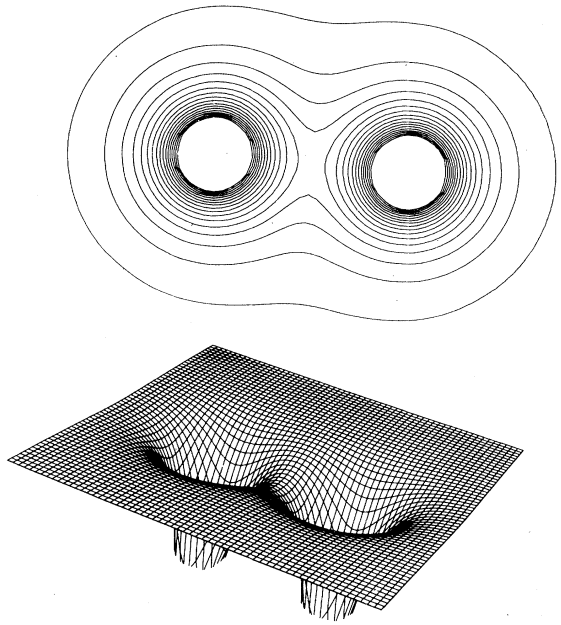

FIG. 2. The total FLAPW potential for the O_2 molecule, including the Coulomb potential and the exchange-correlation potential. The outermost contour is at −0.8 Ry, which is also the contour spacing. The cutoff in the figure is at −13.6 Ry.

pseudopotential calculation for O_2, differ from the results shown in Fig. 3 in the following features: Near the nuclei the $2\sigma_g$ and $2\sigma_u$ densities have a nodal structure which is not described in the pseudopotential (PP) approach. In the PP result, the $3\sigma_g$ density has two peaks, in the bonding between the atoms, which are much closer and broader than those in our calculation; furthermore, the kidney-shaped outer maxima that we find is not present in the PP result. The maxima of $1\pi_u$ and $1\pi_g$ densities are closer to the nuclei in our calculation compared with the PP densities.

D. Accuracy of the FLAPW eigenvalues

Here we discuss and assess the accuracy of our new FLAPW method by comparing the energy eigenvalues of the one-particle local-density equations with those obtained[13,14] by state-of-the-art LCAO-type calculations using the discrete variational method[17] and by a pseudopotential calculation.[16] In comparing results, the type and convergence of the basis used must be considered. For an LCAO-type basis, it is difficult to show that it is sufficiently converged.[18] Increasing the number of atomic orbitals included in the LCAO basis may not change the result markedly and one may still be far from describing the given molecular orbital adequately. In contrast, the FLAPW basis allows one to easily monitor the convergence in the number of basis functions used. Therefore special attention is paid to this point when comparing the FLAPW and DVM eigenvalues.

The first LCAO-DVM calculation for the O_2 molecule within local-density functional theory was performed by Baerends and Ros[14] using double-zeta Slater-type atomic orbitals to construct the molecular wave functions. The resulting eigenvalues (labeled DVM-1 in Table II and Fig. 4) are in good overall agreement with the FLAPW results. It should be noted that our eigenvalues are given with respect to the vacuum potential, i.e., they are not shifted in any way. The most significant difference between the DVM-1 and FLAPW eigenvalues is that the FLAPW splitting between the bonding $2\sigma_g$ and antibonding $2\sigma_u$ states originating from the atomic $2s$ functions is smaller by 0.108 Ry. The positions of the $1\pi_g$ and $1\pi_u$ in the two calculations differ by less than 0.006 Ry.

In 1979, Kerker *et al.*[16] published results of a self-consistent pseudopotential calculation for O_2 using a solid-state approach in the form of a three-dimensional supercell. Comparison of the PP and the FLAPW eigenvalues (see Table II and Fig. 4) shows a similar splitting of the $2\sigma_g$ and $2\sigma_u$ states. The PP $1\pi_g$ state, however, is too high in energy by 0.107 Ry which is almost 30% of the energy eigenvalue itself.

This discrepancy in the highest occupied valence states may be due to the truncation of the basis used in the PP calculation. The convergence of the FLAPW eigenvalues obtained with the self-consistent potential by truncating the number of

basis functions per symmetry from about 350 to about 100 is displayed in Fig. 5. The left-hand side of Fig. 5 shows the PP eigenvalues[16] shifted so that the converged $2\sigma_g$ eigenvalues coincide. [For purposes of comparison with the DVM-1 (Ref. 14) results, it appears that the PP eigenvalues[16] were shifted so as to align the $2\sigma_g$ levels. Such a shift seems to be necessary since the 3D-supercell method,being a bulk method, does not define a strict zero of energy.] The agreement between the PP and FLAPW results for the splitting of the rapidly converging $2\sigma_g$ and $2\sigma_u$ states is excellent, in fact, better than the agreement with the DVM results. A comparison of the more extended (and slower converging) $3\sigma_g$, $1\pi_u$, and $1\pi_g$ states, however, suggests that the PP basis was too truncated for sufficient variational freedom. Although both FLAPW and the mixed-basis PP used in Ref. 16 are plane-wave—based methods, a direct comparison of the number of basis functions is difficult since FLAPW is an all-electron method while the PP method is not. An added difficulty faced in a a 3D-supercell method is that more $\vec{k}$ vectors, i.e., basis functions, are needed to fill up $\vec{k}$ space to a given maximum k compared to the slab geometry used here.

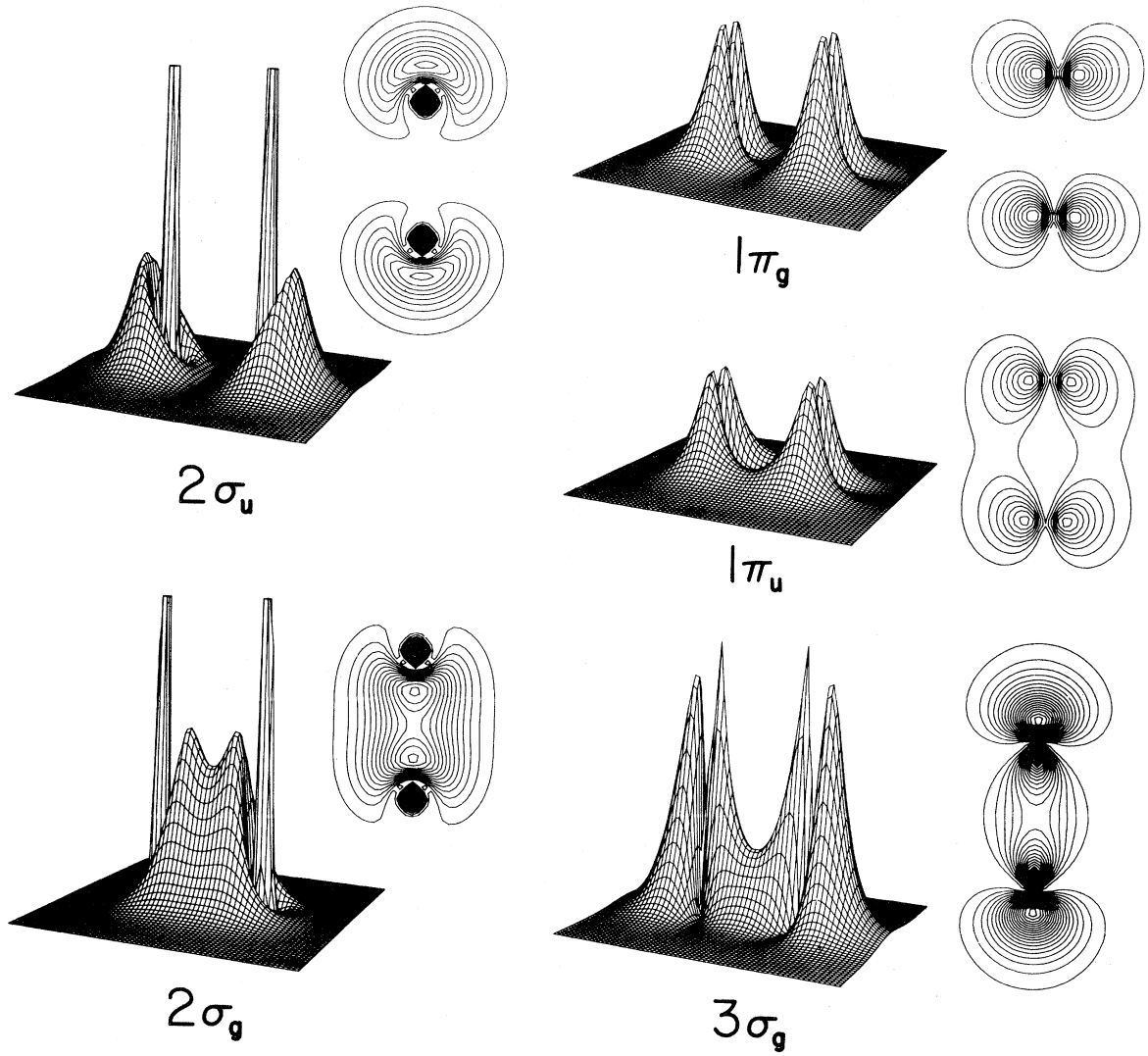

FIG. 3. Densities for the occupied valence states in the O_2 molecule for a cut in a plane containing the two nuclei. Each single-state density is normalized to unity. The values of the lowest contour lines and also the contour spacings are 0.016 electrons/(a.u.)^3.

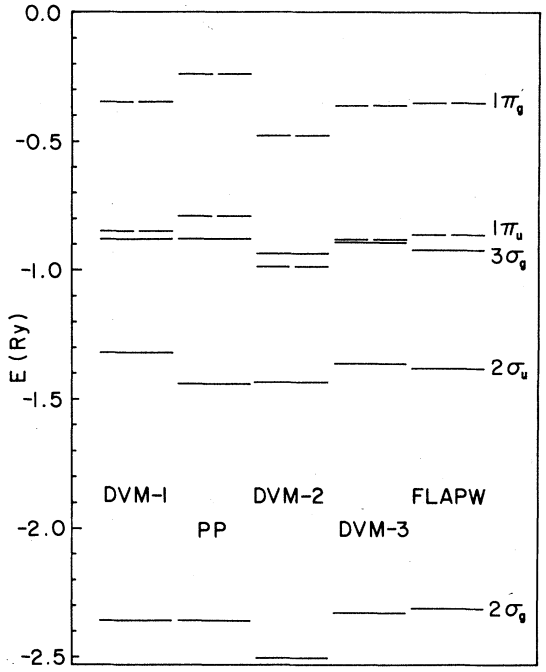

FIG. 4. Local-density energy eigenvalues for O_2 obtained by self-consistent calculations. DVM-1 denotes the discrete variational method results by Baerends and Ros (Ref. 14), PP refers to a pseudopotential calculation given by Kerker *et al.* (Ref. 16), and DVM-2 and DVM-3 label the Delley *et al.* results (Ref. 13) obtained with the discrete variational method using a small two-center basis (DVM-2) and a two-center basis extended by 48 off-site functions. The last column gives the full-potential linearized-augmented-plane-wave eigenvalues.

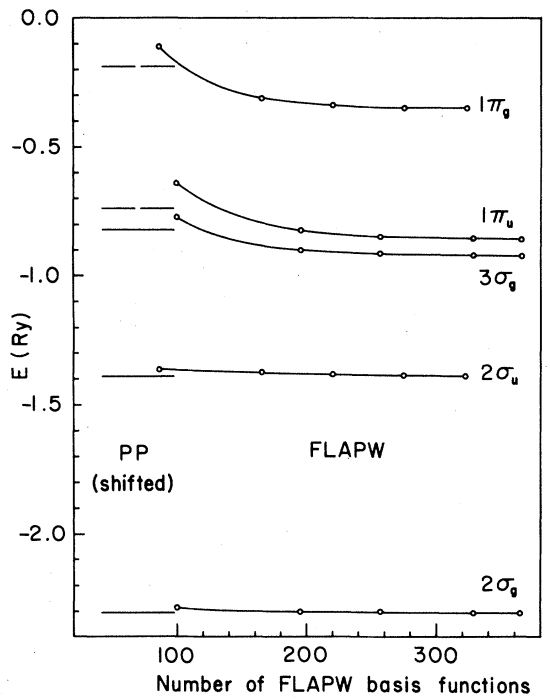

FIG. 5. FLAPW eigenvalues obtained with the self-consistent potential and various basis sets. The pseudopotential results of Kerker *et al.* (Ref. 16) are shifted such that the $2\sigma_g$ states line up with the FLAPW values.

E. Comparison with recent LCAO-DVM calculations

Figure 4 also presents the results of two new DVM calculations[13] denoted by DVM-2 and DVM-3. The basis used in the DVM-2 calculation consists of a linear combination of atomic functions with $l \leq 2$ obtained for the free oxygen atom using the same form of the local exchange correlation, i.e., $X\alpha$, with $\alpha = 0.7$, as in the molecular calculation. The large discrepancy between the DVM-2 eigenvalues and the FLAPW results clearly provokes further investigation.

TABLE II. Local-density energy eigenvalues for the O_2 molecule. DVM-1 refers to the results of Baerends and Ros (Ref. 14), PP labels the pseudopotential results given bv Kerker *et al.* (Ref. 16), DVM-2 are the results of a DVM calculation (Ref. 13) using a small two-center basis with $l \leq 2$, and DVM-3 refers to a DVM calculation (Ref. 13) with a two-center basis with $l \leq 2$ extended by 48 off-site functions. The FLAPW eigenvalues are given in the last column.

	O_2 Eigenvalues (Ry)				
	DVM-1	PP	DVM-2	DVM-3	FLAPW
$1\pi_g$	−0.345	−0.243	−0.476	−0.361	−0.350
$1\pi_u$	−0.853	−0.794	−0.984	−0.881	−0.859
$3\sigma_g$	−0.882	−0.875	−0.935	−0.891	−0.923
$2\sigma_u$	−1.323	−1.441	−1.435	−1.359	−1.381
$2\sigma_g$	−2.359	−2.359	−2.501	−2.323	−2.309
$1s$			−37.773	−37.565	−37.578

To understand the origin of this difference, we synthesized the self-consistent FLAPW potential onto the DVM point mesh (3000 points) and calculated the DVM eigenvalues and wave functions for this potential (without iterating in the DVM). The resulting eigenvalues are plotted in Fig. 6 together with the FLAPW eigenvalues as a reference. In other words, all eigenvalues given in Fig. 6 are obtained with a common potential but using two radically different methods for representing the molecular wave functions. From Fig. 6 it is obvious that the greatest deviations between DVM-2 and FLAPW eigenvalues are found for the $2\sigma_g$ and $3\sigma_g$ orbitals, i.e., just those orbitals which have their greatest density in the bonding region (see Fig. 3). The fact that the $2\sigma_g$ — DVM-2′ eigenvalues are higher in energy than the corresponding FLAPW eigenvalues indicates that there may not be enough variational freedom in the DVM-2 wave functions which are standard two-center expansions in atomic orbitals. Moreover, the inclusion of d functions in the two-center expansion does not change the eigenvalues significantly. Let us focus on the $2\sigma_g$ states. A clue to understanding the difference between the DVM-2 and FLAPW results is certainly given by the charge density. Therefore we have depicted for the $2\sigma_g$ state the difference between the FLAPW and the DVM-2′ charge densities [Fig. 7(a)], where both the DVM-2′ and FLAPW eigenfunctions have been constructed with the common potential underlying Fig. 6, i.e., we have isolated effects which are exclusively due to the different way of constructing the molecular wave function. Figure 7(a) shows now that the DVM-2′ — $2\sigma_g$ wave function is less localized in the bonding region than is the corresponding FLAPW function and points out how to extend the LCAO basis in order to get a significant gain in variational freedom. We can improve the LCAO basis by adding functions centered at points where the difference density has relative maxima, e.g., at the two bumps of the $2\sigma_g$ density between the two nuclei [cf. Figs. 3 and 7(a)]. If this procedure is done for each orbital and the eigenvalues are recalculated for the common FLAPW potential using 48 additional off-center functions, we obtain the results labeled DVM-3′ [Fig. 7(b)]. From Fig. 6 it can be seen that now the DVM-3′ and FLAPW $2\sigma_g$ states line up excellently and that the agreement in the $3\sigma_g$ states is improved significantly. It should be noted that additional DVM functions centered at the middle of the bond do not lead to this agreement, i.e., those functions do not really increase the variational freedom in the present case. The

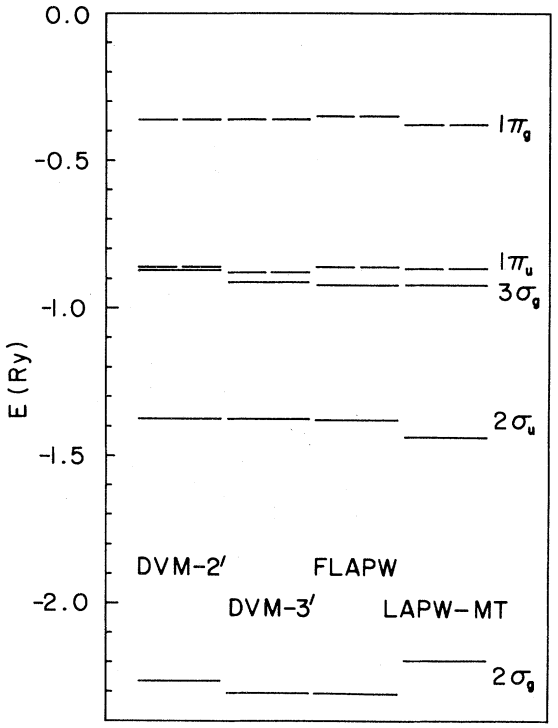

FIG. 6. One-electron energy eigenvalues obtained with a common potential (the full self-consistent FLAPW potential). DVM-2′ and DVM-3′ refer to DVM calculations using small and extended basis sets and LAPW-MT to the FLAPW method when the Hamiltonian matrix elements due to the nonspherical terms in the potential are neglected (warped muffin-tin approximation).

DVM-3′ eigenvalues for the 1π states are slightly lower than the FLAPW values. This may be partly due to residual small interactions between the O_2 molecules in the film geometry and partly due to the somewhat arbitrary way in which the FLAPW potential is continued in the plane of the film to construct a DVM potential which approaches strictly zero also in these directions. In the direction perpendicular to the film, the FLAPW potential already approaches zero in the form required.

Although the energy differences between DVM-2′ and DVM-3′ eigenvalues obtained for the common potential underlying Fig. 6 are small, the real improvement of the DVM basis shows its importance when performing the self-consistent calculation with the extended basis (DVM-3 in Fig. 4). Amazingly, all DVM-3 eigenvalues are shifted to higher energies compared with the DVM-2 results and the DVM-3 eigenvalues are now very close to the FLAPW eigenvalues. The main difference between the original DVM calculation by Baerends and Ros[14]

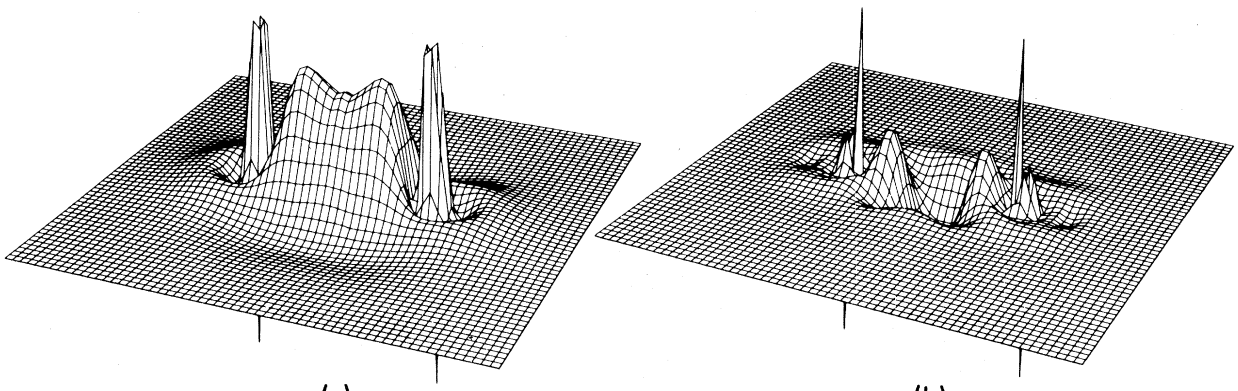

FIG. 7. Difference charge densities for the $2\sigma_g$ states: (a) ρ(FLAPW)-ρ(DVM-2'), and (b) ρ(FLAPW)-ρ(DVM-3') plotted to the same scale. The cutoff in (a) is at 0.2 electrons/(a.u.)^3. All densities are obtained using the same potential (i.e., the full self-consistent FLAPW potential).

(DVM-1) and the new DVM-3 results consists in the splitting of the $2\sigma_g$ and $2\sigma_u$ orbitals; the splitting of these states in DVM-3 is much closer to the FLAPW result than that in the original DVM calculation by Baerends and Ros.

Finally, the influence of the nonspherical terms in the LAPW Hamiltonian matrix elements is demonstrated in Fig. 6. The column labeled "LAPW-MT" refers to eigenvalues obtained using the full self-consistent FLAPW potential but neglecting the nonspherical terms in the Hamiltonian matrix. As expected, the difference are substantial for the 2σ states but small for the 1π states.

IV. CONCLUSIONS

The validity of shape approximations to the potential in solving the one-particle local-density equations depends strongly on the system considered. In particular, the approximation of spherically symmetric potentials inside the muffin-tin spheres may be justified for close-packed systems, but becomes suspect for open structures.

We have shown in the present work how the linearized-augmented-plane-wave method for thin films can be generalized to treat self-consistently the case of a full potential, i.e., one with no shape approximations. The new scheme used for solving Poisson's equation[10] turns out to be not only elegant in its formulation but also numerically efficient as implemented in the full-potential LAPW method.[19]

The accuracy of the new FLAPW method was demonstrated for the severe test case of the nearly free O_2 molecule which exhibits important nonspherical contributions to the potential inside the muffin-tin spheres. It was found that the accuracy of the FLAPW energy eigenvalues and charge densities exceeds that of state-of-the-art LCAO-type calculations within the local-density–functional approach. The FLAPW results can therefore be used as a reference to improve the standard LCAO basis by adding off-site variational functions in those regions of space found appropriate by comparing the two sets of results.

Thus the FLAPW method is ideally suited to treat the electronic structure of reduced symmetry systems such as semiconductor surfaces, interfaces, or molecules chemisorbed on metal surfaces. FLAPW is a unified method in the sense that it can describe not only chemisorbed systems but also the isolated components of such a system, namely the clean surface and the nearly free molecule, to the same precision.

ACKNOWLEDGMENTS

We are grateful to B. Delley and D. E. Ellis for close cooperation on the DVM-LCAO and FLAPW comparisons and to D. R. Hamann for suggesting the basic method for solving Poisson's equation and for an iteration scheme in the self-consistency procedure. This work was supported by the National Science Foundation (Grant No. DMR77-23776 and under the NSF-MRL program through the Materials Research Center of Northwestern University, Grant No. DMR79-23573) and the Department of Energy. We thank M Division of Lawrence Livermore Laboratory for their support in the use of the MFE CRAY computer.

APPENDIX: THE STAR-FUNCTION EXPANSION OF THE DIFFERENCE PSEUDO-CHARGE-DENSITY

The pseudo-charge-density is expressed as

$$\tilde{\rho}_{n,s} = \rho_{n,s}^{\mathrm{PW}} + \Delta\tilde{\rho}_{n,s} \ , \tag{A1}$$

where $\rho_{n,s}^{\mathrm{PW}}$ are the star-function expansion coefficients of the interstitial charge [Eq. (1b)]. The coefficients of the difference pseudo-charge-density, $\Delta\tilde{\rho}_{n,s}$, depend on the multipole moments of the original charge density and the plane-wave charge density as follows:

$$\Delta\tilde{\rho}_{n,s} = \frac{2\pi}{\Omega}\frac{D}{D'} m_s (2-\delta_{k_n,0}) \sum_{\alpha}\sum_{\nu} R^{\alpha}_{n,s,\nu} \frac{1}{n_0} \sum_{R} \exp(i\hat{R}\vec{G}_s\cdot\vec{t}_R) Q^{\alpha}_{\nu}(\hat{R}\vec{G}_s,\vec{k}_n) \ , \tag{A2}$$

with

$$\mathfrak{R}^{\alpha}_{n,s,\nu} \equiv \prod_{\mu=0}^{N} (2l_\nu + 3 + 2\mu) R_\alpha^{-l_\nu} (K_{ns}R_\alpha)^{-(N+1)} j_{l_\nu+N+1}(K_{ns}R_\alpha) \tag{A3}$$

and

$$Q^{\alpha}_{\nu}(\hat{R}\vec{G}_s,\vec{k}_n) \equiv \sum_{m} [(-1)^{l_\nu+m} F^{\alpha}_{\nu}(\hat{R}\vec{G}_s - \vec{k}_n) + F^{\alpha}_{\nu}(\hat{R}\vec{G}_s + \vec{k}_n)] \overline{q}^{\alpha}_{l_\nu m} Y_{l_\nu m}(\hat{R}\vec{G}_s + \vec{k}_n) \ , \tag{A4}$$

$$F^{\alpha}_{\nu}(\hat{R}\vec{G}_s \mp \vec{k}_n) \equiv \begin{cases} (-1)^{l_\nu/2} \cos[(\hat{R}\vec{G}_s \mp \vec{k}_n)\cdot\vec{\tau}_\alpha] & \text{for } l_\nu \text{ even} \quad \text{(A5a)} \\ (-1)^{(l_\nu+1)/2} \sin[(\hat{R}\vec{G}_s \mp \vec{k}_n)\cdot\vec{\tau}_\alpha] & \text{for } l_\nu \text{ odd} \ , \quad \text{(A5b)} \end{cases}$$

$$\overline{q}^{\alpha}_{l_\nu m} = q^{\alpha}_{l_\nu m} - q^{\mathrm{PW}\alpha}_{l_\nu m} \ . \tag{A6}$$

Ω is the volume of the unit cell between the vacuum boundaries at $\pm D/2$. $D' > D$ is used to define $\vec{k}_n$, reciprocal-lattice vector in the z direction [Posternak *et al.*,[4] Eq. (2)]. m_s denotes the number of members in the star of $\vec{G}_s$, a 2D star representative. α denotes an atom in the unit cell at position $\vec{\tau}_\alpha$. ν is a label of a lattice harmonic with the l value l_ν. $\{\hat{R} \mid \vec{t}_R\}$ forms the 2D space group of order n_0. N, the "convergence parameter," is an arbitrary integer greater than 0 chosen such that for a maximum $K_{ns}R_\alpha$ the Fourier series for $\Delta\tilde{\rho}$ converges most rapidly.[10] In our case $K_{ns}R_\alpha = (|\vec{G}_s| + |\vec{k}_n|)R_\alpha \leq 15$, so we used $N = 9 - l$. R_α is the muffin-tin radius of sphere α.

The multipole moments of the original charge density [given by Eq. 1(a)] are

$$q^{\alpha}_{l_\nu m} = c^{\alpha}_{m}(l_\nu) \int_0^{R_\alpha} \rho_\nu(r) r^{l_\nu+2} dr \tag{A7}$$

and the multipole moments of the plane-wave density inside sphere α are found to be

$$q^{\mathrm{PW}\alpha}_{l_\nu m} = 2\pi i^{l_\nu} \sum_{n,s} \rho^{\mathrm{PW}}_{n,s} R_\alpha^{l_\nu+3} (K_{ns}R_\alpha)^{-1} j_{l_\nu+1}(K_{ns}R_\alpha) \frac{1}{n_0} \sum_{R} \exp[i\hat{R}\vec{G}_s\cdot(\vec{\tau}_\alpha - \vec{t}_R)] \mathcal{Y}^{\alpha,n,s}_{l_\nu m} \ , \tag{A8}$$

with

$$\mathcal{Y}^{\alpha,n,s}_{l_\nu m} \equiv [e^{ik_n\tau_{\alpha z}} + (-1)^{l_\nu+m} e^{-ik_n\tau_{\alpha z}}] Y^{*}_{l_\nu m}(\hat{R}\vec{G}_s + \vec{k}_n) \ . \tag{A9}$$

---

*Permanent address: Inst. f. Techn. Elektrochemie, Technical University, Getreidemarkt 9, A-1060 Vienna, Austria.

[1]W. Kohn and L. J. Sham, Phys. Rev. 140, A1133 (1965).
[2]D. D. Koelling and G.O. Arbman, J. Phys. F 5, 2041 (1975); O. K. Andersen, Phys. Rev. B 12, 3060 (1975).
[3]H. Krakauer, M. Posternak, and A. J. Freeman, Phys. Rev. B 19, 1706 (1979).
[4]M. Posternak, H. Krakauer, A. J. Freeman, and D. D. Koelling, Phys. Rev. B 21, 5601 (1980).
[5]H. Krakauer, M. Posternak, and A. J. Freeman, Phys.

Rev. Lett. 43, 1885 (1979); 41, 1072 (1978); D.-S. Wang, A. J. Freeman, H. Krakauer, and M. Posternak, Phys. Rev. B 23, 1685 (1981).
[6]O. Jepsen, J. Madsen, and O. K. Andersen, Phys. Rev. B 18, 605 (1978).
[7]H. Krakauer, M. Posternak, A. J. Freeman, D. D. Koelling, Phys. Rev. B 23, 3859 (1981).
[8]D.-S. Wang, H. Krakauer, and A. J. Freeman (unpublished).
[9]D. R. Hamann (private communication); Phys. Rev. Lett. 42, 662 (1979).
[10]M. Weinert, J. Math. Phys., in press.
[11]J. A. Appelbaum and D. R. Hamann, Phys. Rev. B 6, 2166 (1972).
[12]J. D. Jackson, *Classical Electrodynamics,* 2nd ed. (Wiley, New York, 1975).
[13]B. Delley, D. E. Ellis, and A. J. Freeman (unpublished).
[14]E. J. Baerends and P. Ros, Chem. Phys. 2, 52 (1973).
[15]A. C. Wahl, Science 151, 961 (1966).
[16]G. P. Kerker, A. Zunger, M. L. Cohen, and M. Schlüter, Solid State Commun. 32, 309 (1979).
[17]D. E. Ellis and G. S. Painter, Phys. Rev. B 2, 2887 (1970).
[18]H. Eschrig and I. Bergert, Phys. Status Solidi B 90, 621 (1978).
[19]The recently published results of Monkhorst and Schwalm (MS) [Phys. Rev. B 23, 1729 (1981)] and the possibility of generalizing their work on the total electrostatic energy of a periodic film of atoms in order to treat the full Coulomb potential have been brought to our attention. In comparison with our method, the method of MS requires the use of the (extremely slowly converging) Fourier representation of the total (including core) electronic charge density [Eqs. (60), (A33), and (A34)] and the calculation of real-space lattice sums [Eq. (A32)]. This choice allows one to use the same representations everywhere in space, as opposed to our use of the "natural" representations in the different regions of space, but makes the calculations unfeasible.